Transactions, SMiRT-23
Manchester, United Kingdom - August 10-14, 2015
Division VI, Paper ID 748

MEASUREMENT OF FRICTION COEFFICIENT OF POST-TENSIONING SYSTEM USING SMART STRAND

Se-Jin Jeon[1], Sung-Yong Park[2], Sang-Hyun Kim[3], Hae-Keun Seo[4], Sung-Tae Kim[5], and Young-Hwan Park[6]

[1] Professor, Ajou University, Korea
[2] Research Fellow, Korea Institute of Civil Engineering and Building Technology, Korea
[3] Doctoral Course, Ajou University, Korea
[4] Master's Course, Ajou University, Korea
[5] Chief Researcher, Korea Institute of Civil Engineering and Building Technology, Korea
[6] Senior Research Fellow, Korea Institute of Civil Engineering and Building Technology, Korea

ABSTRACT

Reliable measurement of prestressing force in the post-tensioning system of a prestressed concrete (PSC) structure is very important to maintain the stress level of concrete within allowable limits and to ensure structural safety for an extreme case. Nuclear containment building is a representative PSC structure that has a number of prestressing tendons in hoop and meridian directions, and thus the management of the prestressing force is a crucial part during the service life of the structure including in-service inspection. However, existing management system of the prestressing force of 7-wire strands arranged in a nuclear containment building can only provide limited data on the distribution of prestressing force mainly because there are usually no sensors installed along the length of a tendon. In order to overcome the drawbacks of the existing measurement system, a recently developed Smart Strand system could be a promising solution. In the Smart Strand, the core wire of a 7-wire strand is replaced by carbon fiber reinforced polymer (CFRP) where the fiber Bragg grating (FBG) sensors are built-in. The distribution of prestressing force can be reasonably estimated by the strains measured by a Smart Strand. As one of the applications of the Smart Strand, friction coefficients of post-tensioning system were investigated by the full-scale test of a PSC structure. The test variables were curvature, diameter, and filling ratio of a sheath. The wobble and curvature friction coefficients usually used in the design of a containment building are verified by the analysis of the test results.

INTRODUCTION

Nuclear containment building is a representative prestressed concrete (PSC) structure that has a number of prestressing tendons in hoop and meridian directions, and thus the management of the prestressing force is a crucial part during the service life of the structure including in-service inspection. Therefore, reliable measurement of prestressing force in the post-tensioning system of a containment building is very important to maintain the stress level of concrete within allowable limits and to ensure structural safety for an extreme case. However, existing management system of the prestressing force of 7-wire strands arranged in a nuclear containment building can only provide limited data on the distribution of prestressing force mainly because there are usually no sensors installed along the length of a tendon.

In order to overcome these drawbacks of the existing measurement system, the Smart Strand with the embedded fiber Bragg grating (FBG) sensors was developed in this study to accurately measure the strain and prestressing force along the strand (KICT, 2013; Kim et al., 2015). As one of the applications of the Smart Strand, friction coefficients were evaluated by the full-scale test of a 20 m long beam in this study. Calculation and control of elongation and prestressing force during tensioning of the tendons are of primary importance in post-tensioned concrete structures. In this respect, the friction that occurs through

the interaction between strands and a sheath during tensioning in the post-tensioning system has a significant effect on the distribution of prestressing force and elongation of tendons. The obtained friction coefficients were compared with those specified in current provisions for verification and, as a result, several improvements were proposed.

FRICTION COEFFICIENT

While the prestressing tendons are tensioned using a jack, the loss of prestress occurs along the tendons due to the friction between the tendons and the sheath in post-tensioning system. Figure 1 demonstrates two major sources of the friction. Curvature friction is induced at the curved section of a sheath where the tendons get in contact with the sheath during tensioning. On the other hand, wobble friction occurs even in a straight sheath due to an unintended deformation of the sheath during handling or casting of concrete although the sheath is supported at a certain interval before casting.

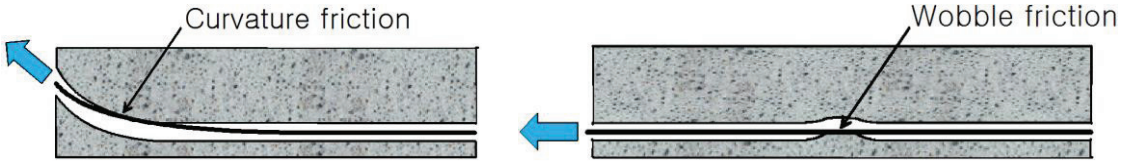

Figure 1. Friction in post-tensioning system.

The predictive equation of the prestressing force as affected by the friction can be derived as in Equation 1 (Nilson, 1987).

$$P_{x1} = P_{x2} e^{-(\mu\alpha + kl)} \tag{1}$$

where,

P_{x1} and P_{x2}: Prestress forces at the points of $x1$ and $x2$ on a tendon, respectively, with $x2$ closer to the tensioning point

μ: Curvature friction coefficient

k: Wobble friction coefficient

α: Variation of angle between $x1$ and $x2$

l: Distance between $x1$ and $x2$

The friction coefficients specified in various codes, specifications, manual, etc. are summarized and compared in Table 1. Although Table 1 represents the case of strands in a galvanized metal sheath that is most frequently used worldwide, it still shows a wide range of variation of the values from provision to provision, and even in a single provision. Therefore, a number of attempts to propose more reasonable friction coefficients have been made so far. However, several studies assumed one of the two types of friction coefficients and evaluated the other friction coefficient (Kitani et al., 2009), which involve intrinsic inaccuracy that strongly depends on the initial assumption of the value of a friction coefficient. Furthermore, some relevant studies referred to the strains measured by conventional electrical resistance strain gauges attached at the surface of a strand. It is generally accepted, however, that the reliability of the strains obtained by this method is quite questionable because of a number of sources of uncertainty and inaccuracy. Therefore, a more reliable methodology is required to derive realistic friction coefficients in term of obtaining the actual strain distribution of a strand and of evaluating the friction coefficients using the measured data.

Table 1: Recommended friction coefficients.

Provisions	Wobble friction coefficient, k (/m)	Curvature friction coefficient, μ (/radian)
Structural concrete design code (KCI, 2012)	0.0015~0.0066	0.15~0.25
ACI 318-08 (ACI, 2008)	0.0016~0.0066	0.16~0.25
ACI 318-14 (ACI, 2014)	Not specified	
Post-tensioning manual (PTI, 2006)	0.0010~0.0023 (Recommended value: 0.0016)	0.14~0.22 (Recommended value: 0.18)
BS 8110 (BSI, 1997)	Not less than 0.0033	0.20, 0.25, 0.30 (Related to rust)
Eurocode 2 (CEN, 2002)	0.00095~0.0019	0.19
fib model code for concrete structures (fib, 2010)	0.0008~0.002	0.16~0.20
Standard specifications for concrete structures (JSCE, 2007)	0.004	0.30

DEVELOPMENT OF SMART STRAND

7-wire strands with a nominal diameter of 12.7 mm or 15.2 mm are usually used as prestressing tendons in PSC structures (ASTM, 2012). It consists of 1 core wire and 6 outer helical wires made of steel as shown in Figure 2(a). When the strain distribution along a strand needs to be measured, there has been no choice but to attach the usual electrical resistance strain gauges on the helical wires exposed outside in most cases, although it is desirable to install the sensors in the straight core wire to minimize the damage caused by the contact between the strands and between the strand and a sheath while tensioning. Moreover, the strain measured from this gauge does not represent an actual axial strain due to the inclination of the helical wires and the difference of the length between the helical wire and the core wire. Damage of the lead wires required for this type of gauge during insertion of strands into a sheath and tensioning is another anticipated problem.

In order to cope with the aforementioned conventional problems, the Smart Strand with the embedded FBG sensors was developed in this study as shown in Figure 2(b) to accurately measure the strain and prestressing force along the strand (KICT, 2013; Kim et al., 2015). In the Smart Strand, the steel core wire of a general strand is replaced with carbon fiber reinforced polymer (CFRP) to contain the optical fiber and Bragg grating sensors at the center of the core wire section. Among several ways to fabricate CFRP, the developed Smart Strand adopted the braidtrusion method to prevent the galvanic corrosion that may occur by the contact with the outer steel helical wires, by virtue of the coated nylon fiber. The principle of the FBG sensor can be found in many references (Nellen et al., 1999). FBG sensors have widely been used recently due to a number of advantages over conventional sensing technique using electrical resistance, such as non-sensitivity to electromagnetic interference, tolerance for extremely low or high temperature, etc. When the light penetrates into an optical fiber, each Bragg grating embedded in the optical fiber reflects the light waves with particular wavelength and transmits all others. By analyzing the reflected light waves, the strain at the point of each Bragg grating can be obtained.

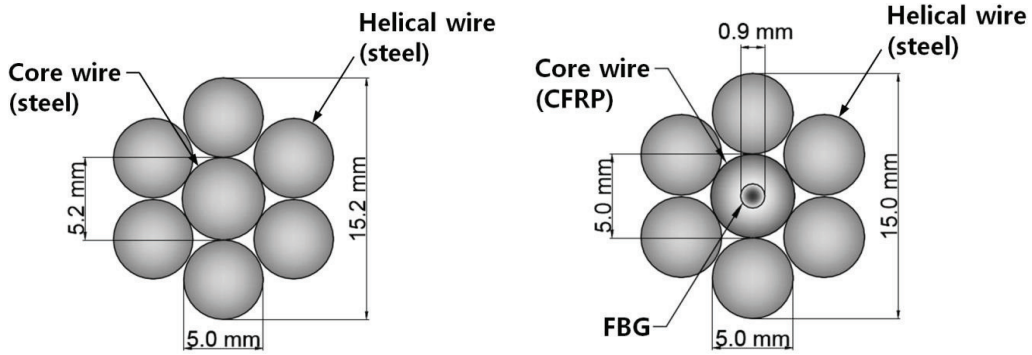

(a) General strand (b) Smart Strand

Figure 2. Comparison of strands.

FULL-SCALE TEST FOR FRICTION COEFFICIENT

Test Specimen and Variables

Test variables were established to include various cases of PSC structures constructed in practice. Test variables of the full-scale test of a PSC beam for evaluating friction coefficients are diameter, curvature, and filling ratio of sheaths as shown in Table 2. 7, 12, and 19 strands are inserted to the sheath with 66 mm, 85 mm, and 100 mm diameter, respectively, in usual cases. However, the effect of the filling ratio on the friction coefficients was also taken into consideration by intentionally reducing the number of strands. Figure 3 shows the 20 m long full-scale test specimen. Specified compressive strength of the specimen is 40 MPa.

The tendons were tensioned at only one end with the opposite end remained as dead end in order to increase friction loss and thus to highlight the friction effect on purpose, although the tendons can also be tensioned at both ends in practice. Total 13 Smart Strands were fabricated, where 6 strands have 7 Bragg gratings and the remaining 7 strands have 5 Bragg gratings that are equally spaced along the length. Among the total number of strands in one sheath, Smart Strands occupied a certain portion and normal strands occupied the remaining portion.

Table 2: Test variables.

Category	Test variables	Values
Sheath	Diameter (mm)	66, 85, 100
	Curvature (sag/length)	0 (straight), 0.0295, 0.0490, 0.0785
	Material	Galvanized metal
Strand	Number	1, 7, 12, 13, 19
	Nominal diameter (mm)	15.2
	Ultimate strength (MPa)	1,860
	Lubrication	Not applied

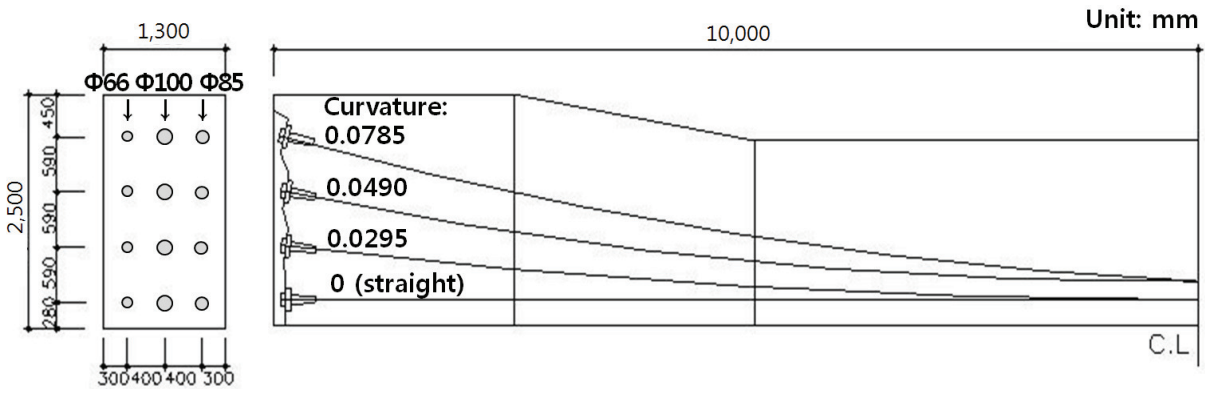

Figure 3. Full-scale test specimen.

Test Results

Figure 4 shows an example of the relationship between jacking force and strains that was obtained in one of the 19 strands inserted in the sheath with diameter=100 mm and curvature=0.0785 in Figure 3. Because the strands were tensioned up to less than the allowable stress, the strains are within an elastic range and thus are almost linearly proportional to the jacking force. The distribution of prestressing force obtained at the same Smart Strand as Figure 4 is presented in Figure 5.

The strains measured at the Bragg gratings of a Smart Strand can be converted to prestress at each grating by multiplying modulus of elasticity of the Smart Strand and can further be converted to prestressing force by multiplying cross sectional area of the Smart Strand. However, the computation of the prestressing force from the strain of the core wire of a Smart Strand can further be refined by accounting for the twist of helical wires and the difference of cross sectional area and material property between the helical wires and the core wire (KICT, 2013).

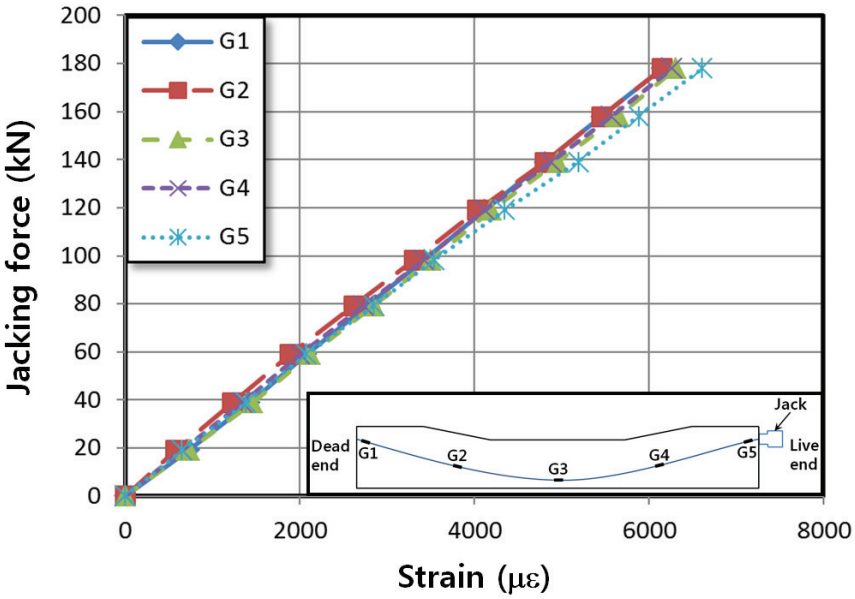

Figure 4. Jacking force-strain relationship.

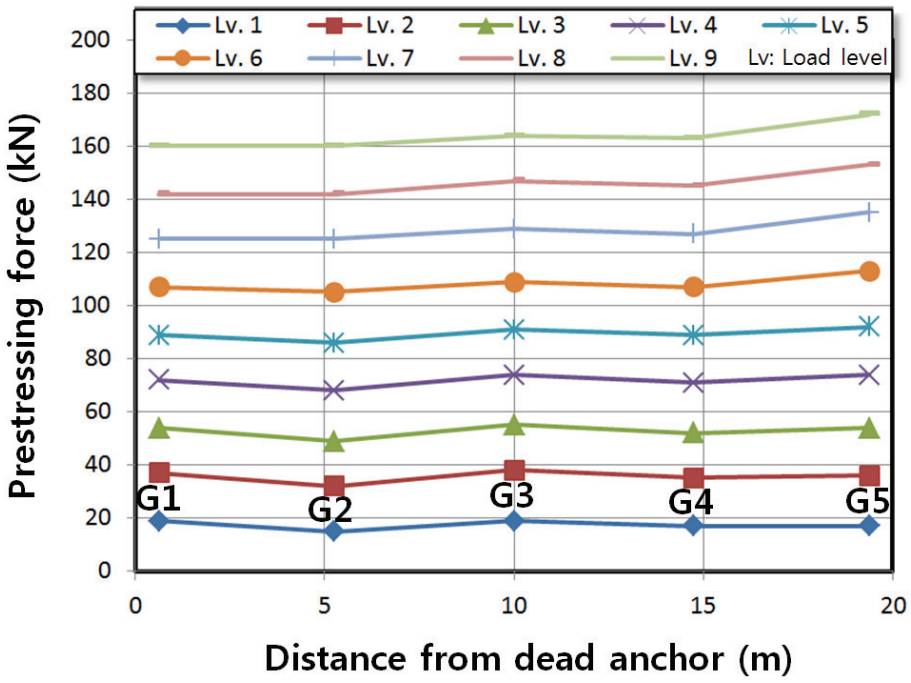

Figure 5. Distribution of prestressing force.

EVALUATION OF FRICTION COEFFICIENTS

Methodology

Friction coefficients can be determined by applying the basic equation shown in Equation 1 and the distribution of prestressing force as presented, for example, in Figure 5. In this study, the friction coefficients were evaluated in two steps for the sheaths with a specific diameter. First, the wobble friction coefficient was evaluated in the straight sheath. Since the variation of angle does not exist in the straight sheath, the wobble friction coefficient can be obtained from two prestressing forces (P_{x1} and P_{x2}) that were arbitrarily selected in a Smart Strand, judging from the form of Equation 1 with the term of $\mu\alpha$ removed. Then, the curvature friction coefficient can be evaluated from Equation 1 by applying two prestressing forces on a curved Smart Strand within a curved sheath with the wobble friction coefficient maintained as the previously obtained value for the straight sheath of the same diameter.

As can be expected, the friction coefficients obtained in such a way vary depending on the two prestressing forces chosen. Therefore, statistical approach is required to derive more reliable friction coefficients. During the statistical process, some of the friction coefficients may exhibit exceptionally high or low values when compared to ordinary range of the coefficients shown in Table 1. It can be attributed to abnormal distribution of prestressing force that can occur in a local region due to excessive twist of strands while inserting or jacking, or inevitable irregularity of alignment of a sheath caused by insufficient support combined by casting pressure of concrete. Therefore, data filtering has been performed for a minority of these exceptional values based on the upper or lower limits of the friction coefficients specified in various provisions of Table 1. As a result, the effective range was assumed as 0.0008~0.0066 /m and 0.14~0.30 /radian for the wobble and curvature friction coefficients, respectively. When the Equation 1 is used to evaluate the friction coefficients, any two arbitrary prestressing forces measured at different points can be adopted

Analysis Results

The results of statistical analyses are presented in Figures 6 and 7 for wobble and curvature friction coefficients, respectively. The average wobble and curvature friction coefficients were evaluated as 0.0038 /m and 0.22 /radian, respectively. Therefore, the wobble friction coefficient was slightly smaller than the average value of 0.0041 /m in Korean standard (KCI, 2012) and ACI 318-08 (ACI, 2008), while the curvature friction coefficient was a little larger than the average value of 0.2 /radian in the Korean standard (KCI, 2012) and 0.21 /radian in ACI 318-08 (ACI, 2008). In general, however, the evaluated values were similar to the average values specified in these provisions. The research significance of this study can be found in direct evaluation of the friction coefficients by utilizing the advanced sensing technology using FBG embedded in a strand.

The confidence level of each friction coefficient was also investigated in Figures 6 and 7. The 95% confidence interval was calculated using the corresponding mathematical equation (Kreyszig, 2011) for each case. The 95% confidence interval marked by gray color in Figures 6 and 7 presents the absolute lower and upper limits that can cover all the cases with sufficient reliability. Through this type of statistical way, a wide range of the friction coefficient specified in a specific provision can be made narrow to enhance the accuracy and reliability. For example, whereas the range of the vertical axes of Figures 6 and 7 corresponds to that of ACI 318-08 (ACI, 2008) and Korean standard (KCI, 2012), the range can be narrowed to 0.0033~0.0043 /m and 0.210~0.244 /radian for wobble and curvature friction coefficients, respectively, by applying 95% confidence level.

In this study, the effect of curvature, diameter, filling ratio of a sheath, and the effect of the location of a strand in a sheath, on the friction coefficients have also been investigated. However, this paper presented the general average friction coefficients in terms of wobble and curvature, taking all the test variables into consideration, as are specified without any limited condition in the most provisions shown in Table 1.

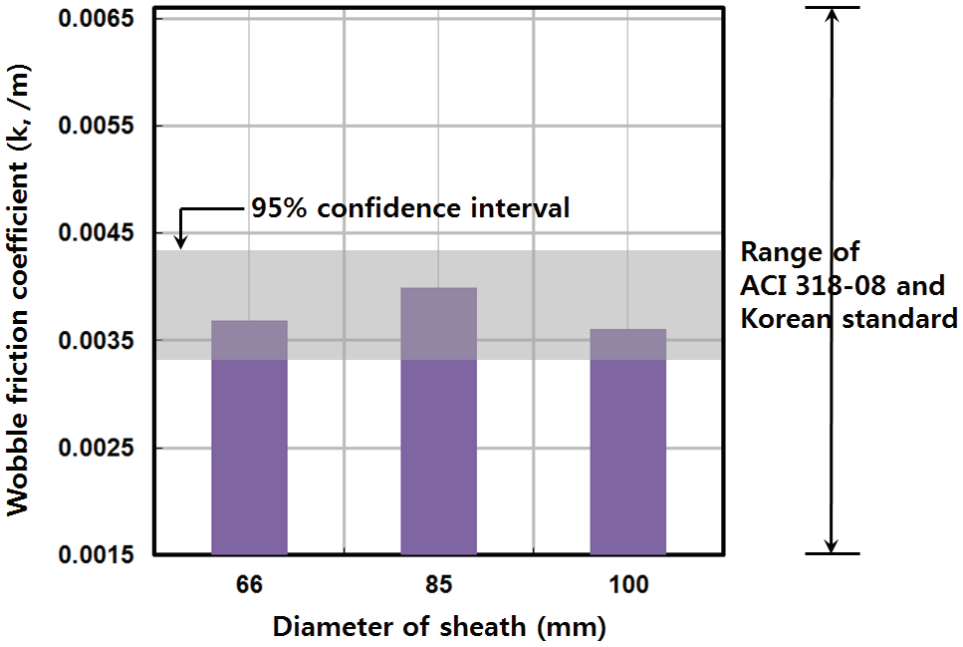

Figures 6. Wobble friction coefficient.

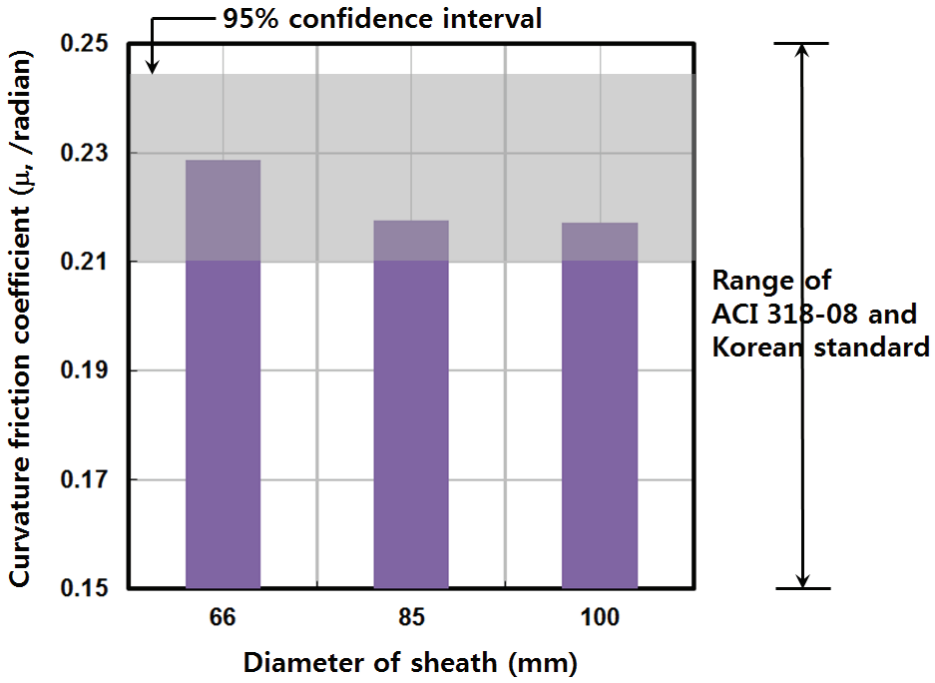

Figures 7. Curvature friction coefficient.

CONCLUSION

In order to overcome several drawbacks of the existing measurement system of the prestressing force of strands in PSC structures, Smart Strand system was developed in this study by devising the core wire made of carbon fiber reinforced polymer with the fiber Bragg grating sensors embedded. As one of the applications of the Smart Strand, friction coefficients were evaluated using the strain distribution of strands obtained by the full-scale test of a 20 m long beam. Based on the results of the foregoing investigation, the following conclusions can be drawn:

(1) The tests were performed for various curvatures, diameters, and filling ratios of a sheath and for various location of a strand inside a sheath to include general cases. The analysis results showed the wobble and curvature friction coefficients of 0.0038 /m and 0.22 /radian on average, respectively, for general galvanized metal sheaths. They are similar to the middle of the range specified in ACI 318-08 and some Korean design codes.

(2) A wide range of friction coefficients specified in general provisions may cause some difficulty and trial-and-error in choosing an appropriate coefficient for design purpose. Through the statistical analyses using a confidence interval, the accuracy of the coefficients was improved by reducing the effective range.

(3) By applying Smart Strand system to reliably estimate the distribution of prestressing force of strands, as has been demonstrated in this study, relevant specifications regarding the design of PSC structures can be verified and improved, if necessary. It is also expected that the Smart Strand system be used for the maintenance or management of PSC structures, such as a nuclear containment building, by long-term monitoring of prestressing force.

ACKNOWLEDGEMENTS

This research was supported by a grant from a Strategic Research Project (Development of smart prestressing system for prestressed concrete bridges) funded by the Korea Institute of Civil Engineering and Building Technology.

REFERENCES

ACI Committee 318. (2008). *Building Code Requirements for Structural Concrete (ACI 318-08)*, ACI (American Concrete Institute), Farmington Hills, Michigan, USA.

ACI Committee 318. (2014). *Building Code Requirements for Structural Concrete (ACI 318-14)*, ACI (American Concrete Institute), Farmington Hills, Michigan, USA.

American Society for Testing and Materials (ASTM). (2012). *Standard Specification for Steel Strand, Uncoated Seven-Wire for Prestressed Concrete (ASTM A416/A416M-12a)*, ASTM, West Conshohocken, Philadelphia, USA.

British Standards Institution (BSI). (1997). *Structural Use of Concrete (BS 8110)*, BSI, London, UK.

European Committee for Standardization (CEN). (2002). *Design of Concrete Structures (Eurocode 2)*, CEN, Brussels, Belgium.

Japan Society of Civil Engineers (JSCE). (2007). *Standard Specifications for Concrete Structures-Design*, JSCE, Tokyo, Japan.

Kim, S. T., Park, Y. H., Park, S. Y., Cho, K. H. and Cho, J. R. (2015). "A sensor-type PC strand with an embedded FBG sensor for monitoring prestress forces," *Sensors*, 15, 1060-1070.

Kitani, T. and Shimizu, A. (2009). "Friction coefficient measurement test on 13MN class tendon of PC strands for prestressed concrete containment vessel (PCCV)," *Proc., 20th International Conference on Structural Mechanics in Reactor Technology (SMiRT 20)*, Paper 1825.

Korea Concrete Institute (KCI). (2012). *Structural Concrete Design Code*, KCI, Seoul, Korea.

Korea Institute of Civil Engineering and Building Technology (KICT). (2013). *Development of Smart Prestressing and Monitoring Technologies for Prestressed Concrete Bridges*, KICT 2013-167, KICT, Goyang-si, Korea.

Kreyszig, E. (2011). *Advanced Engineering Mathematics*, 10th ed., Wiley, Hoboken, New Jersey, USA.

Nellen, P. M., Frank, A., Broennimann, R., Meier, U. and Sennhauser, U. J. (1999). "Fiber optical Bragg grating sensors embedded in CFRP wires," *SPIE Proceedings*, 3670, 440-449.

Nilson, A. H. (1987). *Design of Prestressed Concrete*, Wiley, Hoboken, New Jersey, USA.

Post-Tensioning Institute (PTI). (2006). *Post-Tensioning Manual*, 6th ed., PTI, Phoenix, Arizona, USA.

The International Federation for Structural Concrete (fib). (2013). *fib Model Code for Concrete Structures 2010*, fib, Lausanne, Switzerland.